Low-Speed Aerodynamic Characteristics of Close-Coupled Canard Configuration at Incidence and Sideslip

G. Bandyopadhyay*
Indian Institute of Technology, Kharagpur, 721 302, India

A numerical method has been developed for the prediction of low-speed aerodynamic characteristics of close-coupled canard configurations at zero and nonzero sideslipping angles, taking into consideration the effect of separation along the leading edges of the canard. The method is based on the nonplanar vortex lattice model in which free vortex sheets separating from the leading edges of the canard and trailing edges of both canard and main wing are represented by multiple nonintersecting line vortices. To illustrate the effect of canard leading-edge flow separation, attached flow solutions, based on the vortex-lattice model, are also obtained for zero and nonzero sideslipping angles. To check the accuracy of the separated flow solution, experimental tests have been conducted in a low-speed wind tunnel on a canard model at 0- and 10-deg sideslipping angles. The comparison shows good agreement for both cases up to approximately 16-deg incidence.

Nomenclature

A_{ji} = influence coefficient matrix
B_{ji} = influence coefficient matrix
b = span
C_L = lift coefficient of canard-wing combination based on wing area $S_w = C_{L_w} + (S_c/S_w)C_{L_c}$
C_{L_c} = canard lift coefficient based on canard area S_c
C_{L_w} = wing lift coefficient based on wing area S_w
C_ℓ = rolling moment coefficient
C_M = pitching moment coefficient
c = local chord
$\bar{c}$ = mean aerodynamic chord
$\bar{c}_\ell$ = local lift coefficient
c_R = root chord of canard
M,N = number of spanwise and chordwise divisions of lifting surfaces, respectively
S_c = canard chordal surface area
S_w = wing chordal surface area
s = semispan
U_∞ = freestream speed
u,v,w = perturbation velocity components
V_e = local velocity at the midpoint of a vortex segment
W_j = total downwash at the jth collocation point
α = angle of incidence
β = angle of sideslip
Γ = wing dihedral
$\Delta\Gamma_i$ = vortex strength on ith panel
$|\delta|$ = length of vortex segment
ρ = air density

Subscripts

w = main wing
c = canard

Introduction

CONSIDERABLE aerodynamic benefits can be achieved by placing a vortex generating surface ahead of a lifting wing. One of the most common forms of the vortex generating surface is the canard, which is being used increasingly in the design of modern generation combat aircrafts (e.g., XFV-12A, SAAB Gripen, or European Fighter Aircraft).

The main advantages of canard configurations are observed in an enhancement of lifting capability, particularly at high angles of attack, and in an extension of the lift curve through the stall compared to the canard-off case. This extension of the linear characteristics is due to a delay of the bubble-type separation from the wing surface. This results in a reduction of separation drag and an improved effectiveness of the aft-located control surface.

A significant disadvantage for canard configurations is associated with the problem arising from the presence of free vortices quite close to the configuration surface. This may pose considerable difficulties particularly for the sideslipping motion due to asymmetry in vortex formation. Another disadvantage is related to the problem of vortex breakdown at high angle of attack, which effectively puts an operational limit on such configurations.

To resolve these problems and to get an understanding of the aerodynamic characteristics of the close-coupled canard configuration, a number of experimental studies[1-10] have been conducted for the past three decades. However, the availability of theoretical models for such configurations, even for the symmetric problem, is not so common. The difficulty in developing theoretical models seems to get the canard-induced vortex field represented properly as it passes over the wing since the strength, shape, and position of separation vortices are all unknowns.

For a single-wing problem involving separation along leading edges, simplified methods have been developed in the past due to Brown and Michael,[11] Mangler and Smith,[12] and Polhamus.[13] These methods were followed by three-dimensional techniques based on a vortex-lattice model in which separation vortex is represented by multiple line vortices. The various three-dimensional methods[14-18] use a variety of discretization schemes. Rectangular paneling is used by Mook and Maddox[14] and Kandil et al.,[15] whereas in the method developed by Jepps,[16] conical paneling is used. An unsteady vortex lattice model using rectangular paneling was developed by Katz[17] for wings in sideslip and wings having coning motion. A generalized method applicable for both zero and nonzero angles of sideslip was developed by Bandyopadhyay.[18] In this method, streamwise paneling is used because of its wider applicability to arbitrary planform shapes.

With recent advancements in computer hardware and software, efforts[19-21] are being made to solve Euler and Navier-Stokes equations for a more appropriate calculation of leading-edge separated flows. The major advantages of such codes lie in their ability not only to capture the vorticity at a sharp edge or at a smooth surface but also to align the vorti-

Received Dec. 19, 1989; revision received Aug. 17, 1990; accepted for publication Oct. 21, 1990.

*Associate Professor, Department of Aerospace Engineering.

city with streamlines. However, these codes require large computer memory space and long computing time, even for single-wing configurations and an extension to a two-wing arrangement would not perhaps be practicable unless computational resources are very high.

It is primarily because of this reason that attempts have been made to develop prediction methods for canard configuration by extending the vortex lattice models described earlier to a two-wing arrangement. A method has been developed by Kandil[22] by extending the earlier model[15] for single wing in which free vortex is represented by multiple line vortices. Another method has been developed by the Office National d'Etudes et de Recherches Aérospatials (ONERA)[23] in which separation vortex is simulated by multiple point vortices. For delta canard configuration, a simplified method, based on a combination of Brown and Michael's theory[11] and the vortex-lattice concept[24] has been developed by Bandyopadhyay.[9] In this method, the strength and position of separation vortices at the canard trailing edge are computed by the method of Brown and Michael,[11] and the effect of these vortices on the flow over the main wing are calculated by assuming that they pass over this in chordal direction.

An attempt has been made in this paper to develop a prediction method for a close-coupled canard configuration of arbitrary planform shape at incidence and sideslip by extending the earlier method[18] developed for the single-wing problem. The effect of the vortices shed from the canard leading and trailing edges on the wing surface are computed in an iterative manner starting from an assumed initial shape. To make the method applicable for both zero and nonzero angles of sideslip, the entire configuration surface is discretized. Also, the condition argued by Javed and Hancock[25] that for a wing sideslipping to starboard the port tip wing loading should be zero is not satisfied. No significant loss of accuracy will presumably arise due to this, since differences in solution[25] obtained by models with zero and nonzero port wingtip loading are small, particularly for small taper ratio wings.

Computer memory and time requirements for this method are not large and results were obtained using a minicomputer. The method will, therefore, be particularly useful in a preliminary design environment where computational resources are limited and turnaround time on configuration is necessarily short.

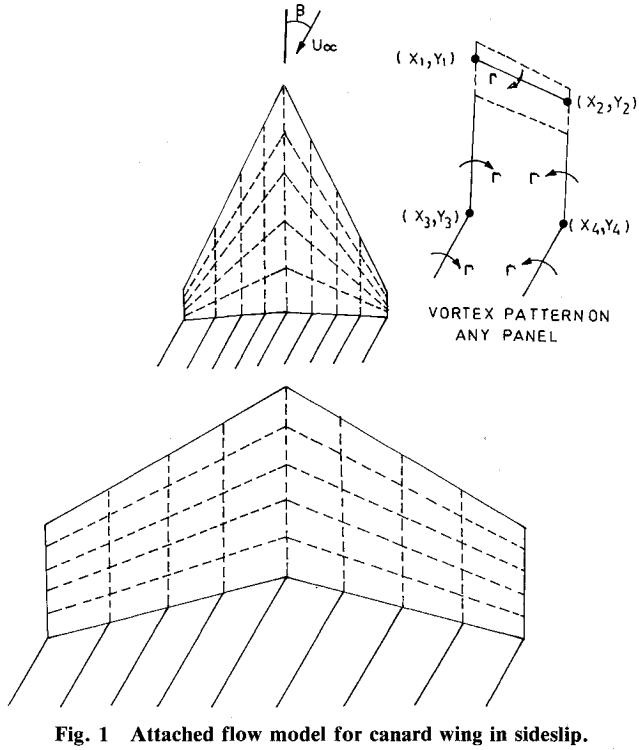

Fig. 1 Attached flow model for canard wing in sideslip.

To evaluate the effect of canard-induced separation vortices, an attached flow model is also developed. Theoretical solutions obtained with attached and separated flow models are compared with experimental values obtained from the wind-tunnel tests of a canard wing model at low speeds. Lift, pitching, and rolling moment estimates are emphasized in the comparison.

Mathematical Model

Attached Flow Model

To illustrate the difference with the separated flow model, the attached flow model is described briefly. In this model, which is based on the planar vortex-lattice theory, both the canard and wing chordal surfaces are divided into a large number of quadrilateral panels. On each panel a horseshoe vortex is placed. The strength of each horseshoe vortex varies from panel to panel. This model with sideslip involves a modification so that the trailing vortices in each panel aft of the trailing edge are taken along the resultant flow direction rather than along the chordal direction (Fig. 1), as shown in Ref. 25 for a single wing. To determine the strengths of the horseshoe vortices $\Delta\Gamma_i$ the boundary condition of zero normal flow is satisfied at all collocation points. This results in a system of simultaneous linear algebraic equations, which can be written in matrix form as

$$[A_{ji}]\{\Delta\Gamma_i\} = \{W_j\} \tag{1}$$

where

$$\begin{aligned} W_j &= -U_\infty\alpha + U_\infty\beta\Gamma \qquad \text{for port wing} \\ &= -U_\infty\alpha - U_\infty\beta\Gamma \qquad \text{for starboard wing} \end{aligned} \tag{2}$$

where U_∞ is the onset flow speed.

Once the system of linear algebraic equations, Eq. (1), is solved, the loading on a single panel can be computed from

$$\Delta F = \rho V_e \times \Delta\Gamma\delta \tag{3}$$

In the asymmetric case, both the bound and trailing vortices on the configuration surface carry lift, and the normal force on each panel can be computed from Eq. (3) as given in Ref. 25 as

$$\Delta F_z = \rho U_\infty \Delta\Gamma\,[(y_2 - y_1) + \beta(x_4 - x_3)] \tag{4}$$

and the lift coefficient of each lifting surface can be obtained by numerical integration as

$$C_{L_c} = \frac{1}{\frac{1}{2}\rho U_\infty^2 S_c} \sum_{i=1}^{N\times M} \Delta F_z \tag{5}$$

$$C_{L_w} = \frac{1}{\frac{1}{2}\rho U_\infty^2 S_w} \sum_{i=1}^{N\times M} \Delta F_z \tag{6}$$

$$C_L = C_{L_w} + \frac{S_c}{S_w} C_{L_c} \tag{7}$$

where (x_1,y_1), (x_2,y_2), (x_3,y_3), (x_4,y_4), are the four corner points of each panel (Fig. 1).

Pitching and rolling moment coefficients and the spanwise load distribution can be calculated similarly by numerical integration, as shown in Ref. 25.

Separated Flow Model

The basic difference of the separated flow model with the attached flow model is in the formation of free vortex sheets along sharp edges where separation occurs, i.e., canard leading and trailing edges and the wing trailing edge. To simulate separation along the canard leading edge, a horseshoe vortex

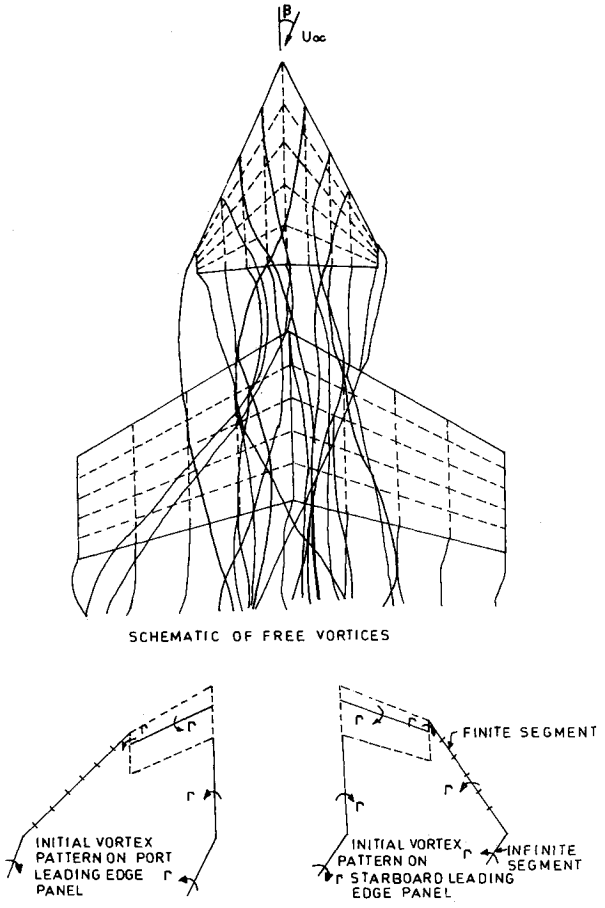

Fig. 2 Separated flow model for canard wing in sideslip.

pattern of each of the N leading-edge panels is modified by suppressing one of the trailing vortices (left one for port panels and right one for starboard panels). Instead of taking it downward to the trailing edge and then to infinity downstream, it is taken upward until it meets the leading edge and is then continued into the fluid to form a free vortex line (Fig. 2). Separation vortex sheets emanating from the canard and wing trailing edges are, likewise, represented by multiple free vortex lines. Each of these free vortex lines is composed of a series of straight line segments, except the last segment, which is semi-infinite extending downstream. The last semi-infinite segment is aligned with the freestream direction; however, the directions of all finite segments are unknowns and are to be calculated iteratively starting from an assumed initial direction. With a prescribed wake shape, the unknown vortex strengths $\Delta\Gamma_i$ are obtained by satisfying the flow tangency condition at collocation points. The set of linear algebraic equations may be given by

$$[B_{ji}]\{\Delta\Gamma_i\} = \{W_j\} \tag{8}$$

where

$$W_j = -U_\infty \sin\alpha \cos\Gamma + U_\infty \cos\alpha \sin\beta \sin\Gamma \text{ for port wing}$$
$$= -U_\infty \sin\alpha \cos\Gamma - U_\infty \cos\alpha \sin\beta \sin\Gamma \text{ for starboard wing} \tag{9}$$

In the subsequent iterations, each finite vortex segment is aligned with the computed velocity at its midpoint, starting at the separation points. In computing the velocity at the midpoint of a finite segment, the influence of the entire vortex line on which that segment lies is ignored, rather than just that of the local segment, as argued by Maskew.[26] With the new wake position, the influence coefficient matrix is recalculated from the flow tangency condition, Eq. (8).

The iteration is terminated when the changes in lift coefficients are $< 2\%$. Convergence is usually quick if the initial direction of free vortex segments is taken as mean flow direction, as argued by Kuchemann,[27] i.e., at an angle $\alpha/2$ to the main stream.

Once the final vortex strengths are known, loading on a single panel can be obtained from Eq. (3), as before. In the nonplanar vortex-lattice model, V_e and δ are given by

$$V_e = U_\infty \cos\alpha \cos\beta \hat{i} - U_\infty \cos\alpha \sin\beta \hat{j} + U_\infty \sin\alpha \hat{k} + u\hat{i} + v\hat{j} + w\hat{k} \tag{10}$$

$$\delta = \delta x\hat{i} + \delta y\hat{j} + \delta z\hat{k} \tag{11}$$

The load carried by each bound vortex segment in each panel can be obtained, as shown in Ref. 24, from Eq. (3) as

$$\Delta F_x = \rho\Delta\Gamma[(-U_\infty \cos\alpha \sin\beta + v)\delta z - (U_\infty \sin\alpha + w)\delta y] \tag{12}$$

$$\Delta F_y = \rho\Delta\Gamma[(U_\infty \sin\alpha + w)\delta x - (U_\infty \cos\alpha \cos\beta + u)\delta z] \tag{13}$$

$$\Delta F_z = \rho\Delta\Gamma[(U_\infty \cos\alpha \cos\beta + u)\delta y + (U_\infty \cos\alpha \sin\beta - v)\delta x] \tag{14}$$

The load carried by each trailing vortex on the configuration surface can be calculated using the previous expressions with suitable modifications. The length of trailing vortex in each panel, δx, is taken as extending from the quarter-chord of the panel to the quarter-chord of the next downstream panel; perturbation velocity components are calculated at the midpoint of this length. Also, δy and δz are both zero in the present streamwise paneling discretization scheme.

Once the total load on each panel is computed by adding the load carried by the bound and two trailing vortices (except the free vortex segments), the resulting lift coefficient of any lifting surface, pitching and rolling moment coefficients can be calculated by numerical integration, as shown in Ref. 24.

Two computer programs have been developed in FORTRAN IV for attached and separated flow models. To make the programs applicable for both zero and nonzero angle of sideslip, the complete configuration surface is discretized. No restriction is imposed on the number of panels in the attached flow model. However, a restriction on the number of spanwise divisions is imposed by Almosnino[28] to prevent the generation of exaggerated induced velocities on the midpoint of a free vortex segment due to the influencing vortex segment next to it. In the separated flow model, the same criterion is used and the optimum lattice of 6×8 is used for each lifting surface. Results are obtained on the Horizon III minicomputer.

Wind-Tunnel Testing

A flat plate canard-wing model has been tested in a low-speed wing tunnel having test section dimensions of 60×90 cm. The canard is a swept wing of aspect ratio 2.9, having a leading-edge sweep of 51.5 deg. The main wing is a moderately swept wing of aspect ratio 3.2 having 29.3-deg sweepback and 10-deg dihedral (Fig. 3). Both canard-on and canard-off configurations have been tested to study the effect of the canard on the flow over the main wing at different angles of incidence and sideslip.

The overall forces and moments were measured by a strain-gauged sting balance using differencing circuits for forces and summing circuits for moments, as described by Bernstein.[29] Data acquisition and reduction were performed using an IBM PC together with an interface circuit employing a 12-bit A/D converter.

Experimental tests were conducted at a Reynolds number of 2×10^5 based on the root chord of the main wing. Correc-

tions due to wind-tunnel interference effect were small and have not been taken into account. A more detailed account of the tests is given in Ref. 30.

Results and Discussion

Variation of lift with incidence, obtained from wind-tunnel testing, is shown in Fig. 4 for both canard-on and canard-off configurations for sideslipping angles of 0 and 10 deg. The advantage of using the canard is observed, for both symmetric and asymmetric flow, in an enhancement of lift, particularly beyond 8 deg. Also, there is an extension of the linearity of the curve for the canard-on configuration due to a delay in bubble-type separation on the wing surface caused by the presence of the canard. Beyond 16 deg, a non-linearity takes place, presumably due to the effects of separation from the wing surface. The figure also indicates the effect of sideslip, which seems to be a slight decrease of lift with sideslip.

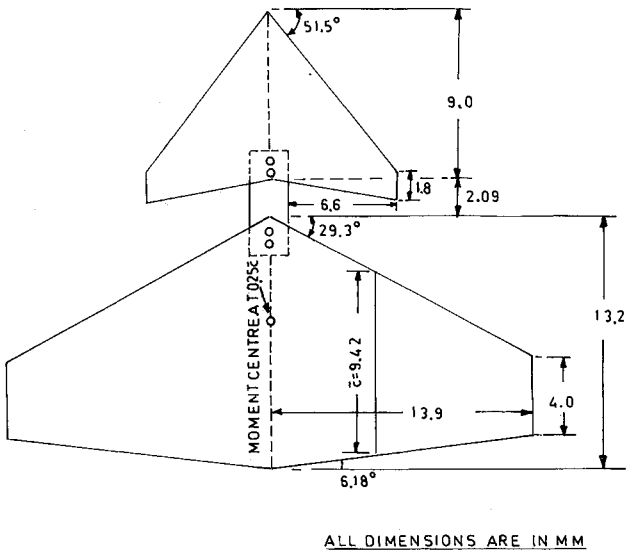

Fig. 3 Canard-wing model for wind-tunnel testing.

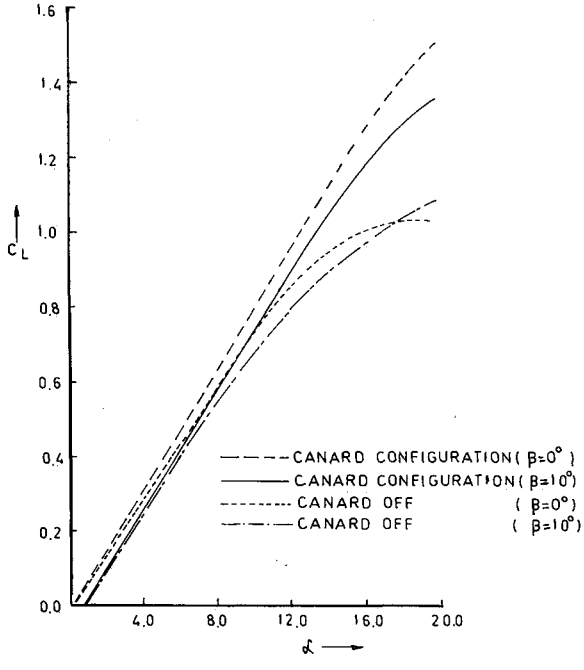

Fig. 4 Comparison of the measured lift coefficients between the canard-off and canard-on configurations for β = 0 and 10 deg.

Figures 5 and 6 show the comparison of theoretical solutions for C_L with experimental values for 0- and 10-deg sideslipping angles, respectively. For both cases, there seems to be good agreement with separated flow solutions except at higher values of incidence where flow separation begins, as indicated by the change in lift-curve slope of the experimental results around 16 deg. This discrepancy beyond 16 deg is due to the fact that the effect of bubble-type flow separation from the wing surface is not taken in the theoretical model.

To illustrate the effect of separation along the canard leading edge, the attached flow solution is also plotted in the same figures. The predicted values of lift are virtually identical up to a 4-deg incidence, beyond which the difference in two solu-

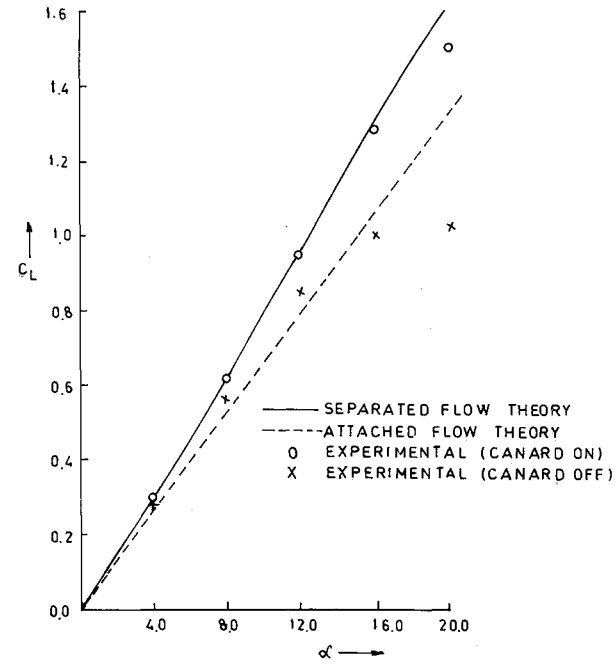

Fig. 5 Comparison of measured and predicted lift coefficients vs α at β = 0 deg.

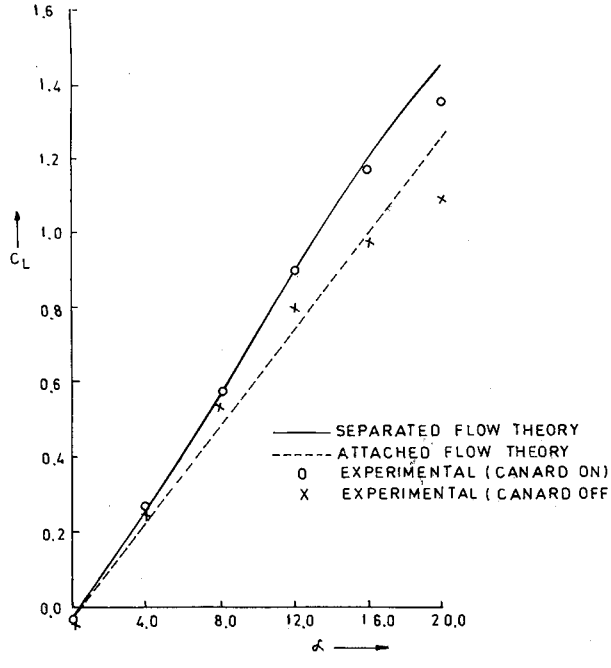

Fig. 6 Comparison of measured and predicted lift coefficients vs α at β = 10 deg.

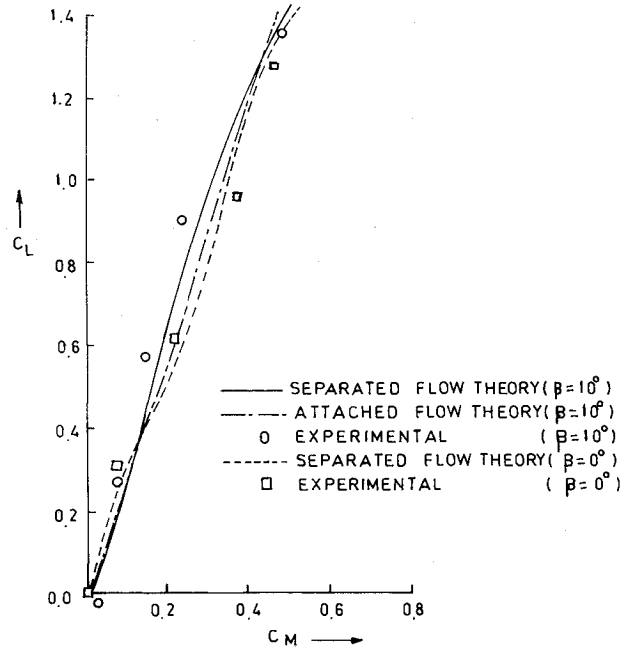

Fig. 7 Comparison of measured and predicted lift coefficients vs pitching moment coefficients for β = 0 and 10 deg.

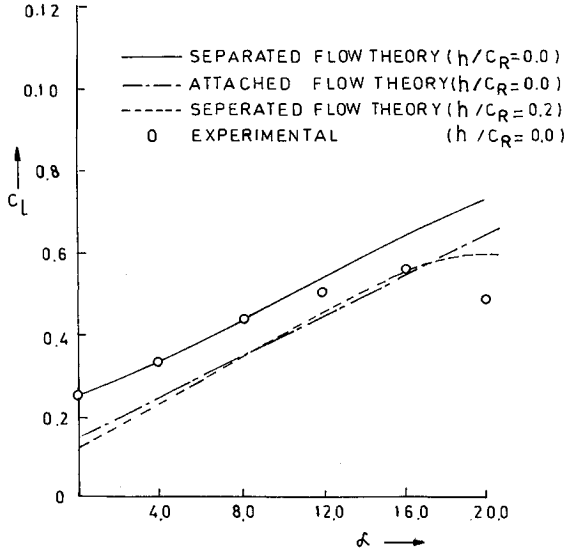

Fig. 8 Comparison of measured and predicted rolling moment coefficients vs α at β = 10 deg.

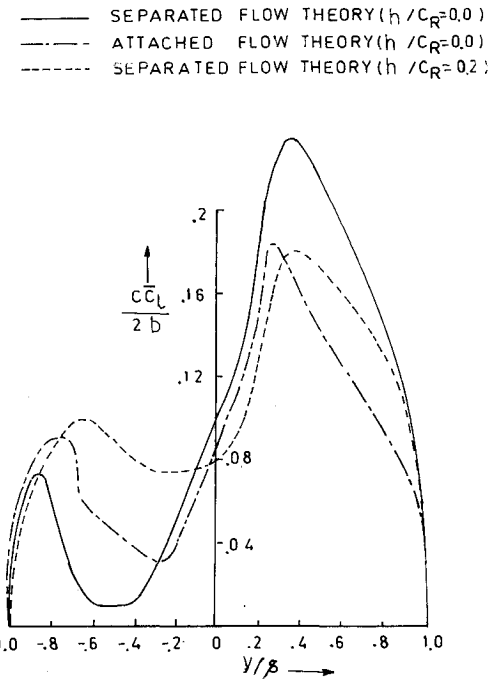

Fig. 9 Predicted spanwise load distribution on main wing at α = 12 deg and β = 10 deg.

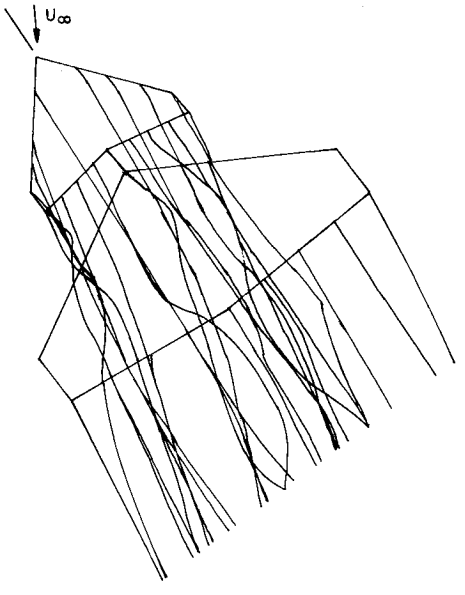

Fig. 10 Pattern of free vortices at α = 12 deg and β = 10 deg.

tions becomes appreciable, indicating the effect of leading-edge separation from the canard.

Both theoretical and experimental results for pitching moment are shown for 0- and 10-deg sideslipping angles in Fig. 7. Pitching moment characteristics appear to be linear, particularly for the zero sideslip case. The comparison of separated flow solutions with experimental values appears to be reasonable. Difference in attached and separated flow solutions (shown for 10-deg sideslip angle) appears to be appreciable beyond 4 deg.

A similar comparison of theoretical solutions with experimental values are shown for rolling moment in Fig. 8. Agreement of the separated flow solution with experimental data is reasonably good, again, except at high incidence. The solution obtained by the attached flow theory, however, shows considerable disagreement, even at low incidence.

Once the accuracy of the separated flow model is established, the effects of horizontal and vertical stagger are studied theoretically. The effect of horizontal stagger seems to be negligible, whereas the effect of vertical stagger seems to provide a marginal increase in lift but a considerable reduction in rolling moment ($-C_\ell$). Variation of the rolling moment coefficient with incidence is also plotted in Fig. 8 for a small vertical stagger (h/c_R) of 0.2.

An explanation of these features can be obtained from the spanwise load distribution for the 10-deg sideslipping angle shown in Fig. 9. The asymmetry in spanwise loading is considerably enhanced in a separated flow solution compared to an attached flow solution due to canard-induced separation vortices leading to an increased loading on the starboard and decreased loading on the port. This results in a considerable increase in the rolling moment coefficient compared to the attached flow solution, whereas the difference in normal force may be relatively small. Similarly, comparison of theoretical solutions for zero and nonzero vertical stagger cases shows that the effect of canard-induced vortices on wing loading is reduced with vertical stagger resulting in a reduction in asymmetry in the spanwise load distribution. As a result of this,

rolling moment is considerably reduced and normal force remains relatively unchanged.

Separation of free vortices from leading edges of the canard and trailing edges of both the canard and the main wing and the subsequent roll up is obtained by using a 6×8 lattice for each lifting surface and is shown in Fig. 10.

Conclusions

Attached and separated flow models have been developed for predicting low-speed aerodynamic characteristics of a canard configuration at various angles of attack and sideslip. To compare the accuracy of theoretical models, wind-tunnel testing has been conducted in a low-speed wind tunnel. A separated flow model is shown to be capable of predicting aerodynamic forces and moments at moderate to high incidence until bubble-type separation occurs. Comparison with the attached flow solution indicates the effects of canard-induced separation vortices.

The experimental and numerical results presented in this paper illustrate some of the general longitudinal and lateral aerodynamics of the canard configuration. Variation of lift with sideslip seems to be small and an advantage of the canard is observed in an enhancement of lifting capability, particularly at high angles and in extending the linearity of the lift-curve slope beyond stall, compared to a canard-off configuration for both zero and nonzero sideslipping angles. The linear characteristics are also observed for pitching and rolling moment for a canard configuration. The effect of horizontal stagger appears to be negligible, whereas the effect of vertical stagger is observed in a marginal increase in lift but a considerable reduction in rolling moment.

Acknowledgment

Research was sponsored by the Aeronautics Research and Development Board, Ministry of Defence, Government of India, New Delhi, under Grant Aero/RD-134/100/10/86-87/450.

References

[1]Behrbohm, H., "Basic Low Speed Aerodynamics of the Short Coupled Canard Configuration of Small Aspect Ratio," Saab, TN-60, Linköping, Sweden, July 1965.

[2]Vogler, R. D., "Ground Effect Investigations of a STOL Air-Sea Transport Model with Blowing Over the Canard and Wing Flaps," NASA TN-D 5988, Oct. 1970.

[3]Dollyhigh, M. S., "Static Longitudinal Aerodynamic Characteristics of Close-Coupled Wing-Canard Configuration of Mach Number from 1.6 to 2.86," NASA TN-D 6597, 1971.

[4]Gloss, B. B., and Mckinny, L. W., "Canard Wing Interference Related to Maneuvering Aircraft at Subsonic Speeds," NASA TM-X-2897, Dec. 1973.

[5]Ray, E. J., and Henderson, W. P., "Low Speed Aerodynamic Characteristics of a Highly Swept Supersonic Transport Model with Auxiliary Canard and High Lift Devices," NASA TM-X-1694, Dec. 1974.

[6]John, H., and Kraus, W., "High Angle of Attack Characteristics of Different Fighter Configuration," AGARD CP-247, 1978, pp. 2-1-2-12.

[7]Kraus, W., "Delta Canard Configuration at High Angle of Attack," *Zeitschrift für Flugwissenschaften und Weltran forschung,* Vol. 7, 1983, pp. 41-46.

[8]Er-El, J., "Effect of Wing/Canard Interference on the Loading of a Delta Wing," *Journal of Aircraft,* Vol. 25, No. 1, 1988, pp. 18-24.

[9]Bandyopadhyay, G., "Low Speed Aerodynamics of Canard Configurations," *The Aeronautical Journal,* Vol. 93, No. 921, 1989, pp. 22-28.

[10]Oelkar, H. C., and Hummel, D., "Investigations on the Vorticity Sheets of a Close-Coupled Delta-Canard Configuration," *Journal of Aircraft,* Vol. 26, No. 7, 1989, pp. 657-666.

[11]Brown, C. E., and Michael, W. H., "On Slender Wings with Leading Edge Separation," NASA TN-3430, April 1955.

[12]Mangler, K. W., and Smith, J. H. B., "A Theory of Slender Delta Wings with Leading Edge Separation," Royal Aircraft Establishment, TN Aero 2442, 1956.

[13]Polhamus, E. C., "A Concept of the Vortex Lift of Sharp-Edge Delta Wings Based on a Leading-Edge-Suction Analogy," NASA TN-D 3767, Dec. 1966.

[14]Mook, D. T., and Maddox, S. A., "Extension of a Vortex Lattice Method to Include the Effects of Leading Edge Separation," *Journal of Aircraft,* Vol. 11, No. 2, 1974, pp. 127-128.

[15]Kandil, O. A., Mook, D. T., and Nayfeh, A. H., "Nonlinear Prediction of Aerodynamic Loads on Lifting Surface," *Journal of Aircraft,* Vol. 13, No. 1, 1976, pp. 22-28.

[16]Jepps, S. A., "The Computation of Vortex Flows by Panel Methods," Von Kármán Institute Lecture Series 5, 1978.

[17]Katz, J., "Lateral Aerodynamics of Delta Wings with Leading Edge Separation," *AIAA Journal,* Vol. 22, No. 3, 1984, pp. 323-328.

[18]Bandyopadhyay, G., "Application of a Vortex Lattice Numerical Model in the Calculation of Inviscid Incompressible Flow around Delta Wings," *International Journal for Numerical Methods in Fluids,* Vol. 10, No. 7, 1990, pp. 729-740.

[19]Fujii, K., Gavali, S., and Holst, T. L., "Evaluation of Navier-Stokes and Euler Solutions for Leading-Edge Separation Vortices," *Numerical Methods in Laminar and Turbulent Flow,* Vol. 5, Pt. 1, Pineridge Press, Swansea, Wales, UK, 1987, pp. 763-774.

[20]Kandil, O. A., and Chuang, A. H., "Influence of Numerical Dissipation on Computational Euler Equations for Vortex-Dominated Flows," *AIAA Journal,* Vol. 25, No. 12, 1987, pp. 1426-1434.

[21]Rizzi, A., and Muller, B., "Large-Scale Viscous Simulation of Laminar Vortex Flow Over a Delta Wing," *AIAA Journal,* Vol. 27, No. 7, 1989, pp. 833-839.

[22]Kandil, O. A., Mook, D. T., and Nayfeh, A., "A Numerical Techique for Computing Subsonic Flow Past Three-Dimensional Canard-Wing Configurations with Edge Separations," AIAA 15th Aerospace Sciences Meeting, AIAA Paper 77-1, Jan. 1977.

[23]ONERA, ACTIVITIES 1981, page 76.

[24]Rubbert, P. E., "Theoretical Characteristics of Arbitrary Wings by a Nonplanar Vortex Method," Boeing Company Rept. D6-9244, 1964.

[25]Javed, M. A., and Hancock, G. J., "Application of Vortex Lattice Methods to Calculate L_v (rolling moment due to sideslip)," Queen Mary College, Rept. EP-1038, England, UK, 1980.

[26]Maskew, B., "Numerical Lifting Surface Methods for Calculating the Potential Flow About Wings and Wing-Bodies of Arbitrary Geometry," Ph.D. Dissertation, Loughborough Univ., 1972.

[27]Kuchemann, D., *The Aerodynamic Design of Aircraft,* Pergamon Press, Oxford, England, UK, 1978, pp. 163.

[28]Almosnino, D., "High Angle-of-Attack Calculation of the Subsonic Vortex Flow on Slender Bodies," *AIAA Journal,* Vol. 23, No. 8, 1985, pp. 1150-1156.

[29]Bernstein, L., "Force Measurement in Short-Duration Hypersonic Facilities," AGARD-AG-214, 1975.

[30]Bandyopadhyay, G., "Stability Characteristics of Canard Wings," Final project report, Aeronautics Research and Development Board, India, 1989.